Inorganic Chemistry

Article

pubs.acs.org/IC

Synthesis of Alkaline Earth Diazenides $M_{AE}N_2$ (M_{AE} = Ca, Sr, Ba) by Controlled Thermal Decomposition of Azides under High Pressure

Sebastian B. Schneider, Rainer Frankovsky, and Wolfgang Schnick*

Department Chemie, Lehrstuhl für Anorganische Festkörperchemie, Ludwig-Maximilians-Universität München, 81377 München, Germany

Supporting Information

ABSTRACT: The alkaline earth diazenides $M_{AE}N_2$ with M_{AE} = Ca, Sr and Ba were synthesized by a novel synthetic approach, namely, a controlled decomposition of the corresponding azides in a multianvil press at high-pressure/high-temperature conditions. The crystal structure of hitherto unknown calcium diazenide (space group *I*4/*mmm* (no. 139), a = 3.5747(6) Å, c = 5.9844(9) Å, Z = 2, wR_p = 0.078) was solved and refined on the basis of powder X-ray diffraction data as well as that of SrN_2 and BaN_2. Accordingly, CaN_2 is isotypic with SrN_2 (space group *I*4/*mmm* (no. 139), a = 3.8054(2) Å, c = 6.8961(4) Å, Z = 2, wR_p = 0.057) and the corresponding alkaline earth acetylenides ($M_{AE}C_2$) crystallizing in a tetragonally distorted NaCl structure type. In accordance with literature data, BaN_2 adopts a more distorted structure in space group *C*2/*c* (no. 15) with a = 7.1608(4) Å, b = 4.3776(3) Å, c = 7.2188(4) Å, β = 104.9679(33)°, Z = 4 and wR_p = 0.049). The N−N bond lengths of 1.202(4) Å in CaN_2 (SrN_2 1.239(4) Å, BaN_2 1.23(2) Å) correspond well with a double-bonded dinitrogen unit confirming a diazenide ion $[N_2]^{2-}$. Temperature-dependent *in situ* powder X-ray diffractometry of the three alkaline earth diazenides resulted in formation of the corresponding subnitrides $M_{AE_2}N$ (M_{AE} = Ca, Sr, Ba) at higher temperatures. FTIR spectroscopy revealed a band at about 1380 cm^{-1} assigned to the N−N stretching vibration of the diazenide unit. Electronic structure calculations support the metallic character of alkaline earth diazenides.

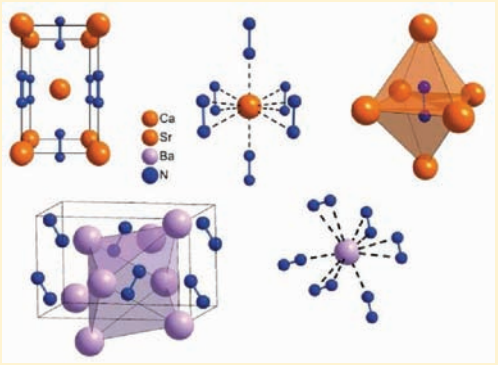

INTRODUCTION

The synthesis and characterization of novel binary metal nitrides have a significant impact on solid-state and materials chemistry due to the numerous applications for such compounds.[1−9] In 2001, the first members of the novel class of nitrogen-rich alkaline earth compounds $M_{AE}N_2$ were discovered and structurally characterized by Kniep et al. revealing dinitrogen anions $[N_2]^{2-}$ with N=N double bonds. The latter anions represent deprotonated diazene N_2H_2 units and were therefore named diazenides. In the past SrN_2 and BaN_2 have been synthesized from the corresponding metals at 620 °C under nitrogen pressure (0.55−0.56 GPa) in a specialized autoclave system.[10−14] Recently, related noble metal nitrides with analogous formula type $M_{NM}N_2$ (M_{NM} = Os, Ir, Pd and Pt) have been synthesized in laser-heated diamond anvil cells in combination with cryogenically loaded nitrogen at high pressure of 50 GPa and temperatures around 2000 °C.[15−23] According to structural and electronic considerations, these noble metal compounds are assumed to contain 4-fold negatively charged nitrogen dimers having the composition $M^{4+}[N_2]^{4-}$.[15−24] Unlike the alkaline earth diazenides, the latter anions (bond length about 1.41 Å)[15−24] are derived from diazane, N_2H_4, containing N−N single bonds and are isosteric with peroxide $[O_2]^{2-}$. Accordingly, these compounds $M^{4+}[N_2]^{4-}$ have been classified as pernitrides,[15−24] and their remarkable properties (e.g., superconductivity, photoluminescence, magnetism and low compressibility comparable to that of c-BN)[15−24] justify the investigation of the crystalline structure, stability, elasticity and electronic structures of the diazenides. However, except for M = Sr, Ba, Os, Ir, Pd and Pt, no other metal diazenides or pernitrides of formula type MN_2 have been synthesized in crystalline form as yet, but have been predicted by density-functional calculations to form under HP/HT conditions.[24−29]

In order to extend the class of nitrogen rich metal diazenides or pernitrides, we have targeted new synthetic approaches for these compounds, and we were successful using controlled decomposition of highly reactive precursors like the corresponding azides. In this contribution, we present our novel synthesis route for the alkaline earth diazenides SrN_2 and BaN_2. In addition, we report on the synthesis, structural, spectroscopic and electronic characterization of the novel alkaline earth diazenide CaN_2 and compare its structure to the predicted model.[26,29]

Received: November 1, 2011
Published: January 11, 2012

   dx.doi.org/10.1021/ic2023677 | *Inorg. Chem.* 2012, 51, 2366−2373

EXPERIMENTAL SECTION

Synthesis of NH_4N_3. Phase-pure NH_4N_3 was obtained by the metathesis reaction of NH_4NO_3 (3.99 g, 50 mmol, Sigma-Aldrich, 99.0%) and NaN_3 (3.25 g, 50 mmol, Acros Organics, Geel, Belgium, 99%) in a silica tube at elevated temperatures. By heating from room temperature to 200 °C within 0.5 h, annealing for 12 h and cooling down again to room temperature within 6 h,[30] NH_4N_3 was precipitated at the cold end of the silica tube separated from $NaNO_3$, which crystallized at the hot end during the reaction.

Synthesis of $Ca(N_3)_2$. Aqueous solutions of calcium azide were obtained from the reaction of $Ca(OH)_2$ with excess of NH_4N_3 (1:4) according to the procedure reported in the literature.[31] First $Ca(OH)_2$ (1.5 g, 20.1 mmol, Sigma-Aldrich, 99.995%) was dissolved in 200 mL of water. Then an excess of NH_4N_3 (4.8 g, 80.5 mmol) was added generating aqueous $Ca(N_3)_2$, NH_3 and H_2O. Ammonia was boiled off, and calcium azide was precipitated by evaporating the water. The calcium azide obtained was dried over $CaCl_2$ (Sigma-Aldrich, 99.99%) using a vacuum desiccator.

Synthesis of $Sr(N_3)_2$ and $Ba(N_3)_2$. Strontium and barium azide were obtained by the reaction of the corresponding hydroxide (Sigma-Aldrich, 99.995%) with an aqueous solution of HN_3, as reported in the literature.[32,33] The extremely dangerous HN_3 was distilled from NaN_3 (Acros Organics, Geel, Belgium, 99%) and H_2SO_4. The solid azides were dried over P_4O_{10} using a vacuum desiccator. A general procedure for the synthesis of the azides of the heavier alkaline earth metals has been described in the literature.[31]

Caution! *Due to the very low thermal and mechanical shock resistance of HN_3, hydrazoic acid should always be handled with maximum caution. Therefore, whenever working with HN_3, efficient protective clothing such as face protections, a leather coat and steel reinforced gloves must be worn.*

Synthesis of $M_{AE}N_2$ (M_{AE} = Ca, Sr, Ba). The three alkaline earth diazenides were synthesized under high-pressure/high-temperature conditions in a modified Walker-type module in combination with a 1000 t press (Voggenreiter, Mainleus, Germany). As pressure medium, precastable MgO-octahedra (Ceramic Substrates & Components, Isle of Wight, U.K.) with edge lengths of 14 or 18 mm (14/8 or 18/11 assembly) were employed. Eight tungsten carbide cubes (Hawedia, Marklkofen, Germany) with truncation edge lengths of 8 or 11 mm compressed the octahedra. The three alkaline earth azides were carefully ground, filled into a cylindrical boron nitride crucible (Henze BNP GmbH, Kempten, Germany) and sealed with a fitting boron nitride plate. Details of the setup are described in the literature.[34−38]

CaN_2 (SrN_2, BaN_2) was synthesized in a 14/8 (18/11, 18/11) assembly which was compressed up to 12 (9, 3) GPa at room temperature within 325 (214, 68) minutes, then heated up to 800 (550, 450) °C in 300 (30, 30) minutes, kept at this temperature for 20 (15, 15) minutes and cooled down to room temperature in 15 (10, 10) minutes. Subsequently, the pressure was released over a period of 958 (623, 183) minutes. The recovered MgO-octahedron was broken apart in a glovebox and the sample carefully isolated from the surrounding boron nitride crucible. A black metallic powder of alkaline earth diazenides was obtained, which is extremely sensitive to moisture.

Powder X-ray Diffraction (PXRD), Structure Solution and Rietveld Refinement. The crystal structures of the three alkaline earth diazenides were analyzed on the basis of powder X-ray diffraction data. The powder diffraction patterns were recorded with a STOE Stadi P powder diffractometer (STOE, Darmstadt, Germany) in Debye−Scherrer geometry using Ge(111) monochromated Mo and Cu Kα_1 radiation (0.7093 Å and 1.54056 Å). For the alkaline earth diazenides of strontium and barium the resulting powder X-ray diffraction patterns fit perfectly the ones reported in the literature.[10−14] In the case of the novel diazenide of calcium, the indexing resulted unambiguously in a tetragonal unit cell with a = 3.57 Å and c = 5.98 Å. A Rietveld refinement (Figure 1) was performed with the TOPAS package[39] using the structure of SrN_2 as starting model. The reflection profiles were determined using the fundamental parameter approach[40] by convolution of appropriate source emission profiles with axial instrument contributions and crystalline microstructure effects. Preferred orientation of the crystallites was described with a spherical harmonics of fifth order. The relevant crystallographic data for the three alkaline earth diazenides and further details of the data collection are summarized in Tables 1 and 2. Further information of the crystal structures may be obtained from the Fachinformationszentrum Karlsruhe, 76344 Eggenstein-Leopoldshafen, Germany (fax, (49) 7247-808-666; e-mail, crysdata@fiz-karlsruhe.de) on quoting the depository numbers CSD-423721 (CaN_2), CSD-423722 (SrN_2) and CSD-423723 (BaN_2).

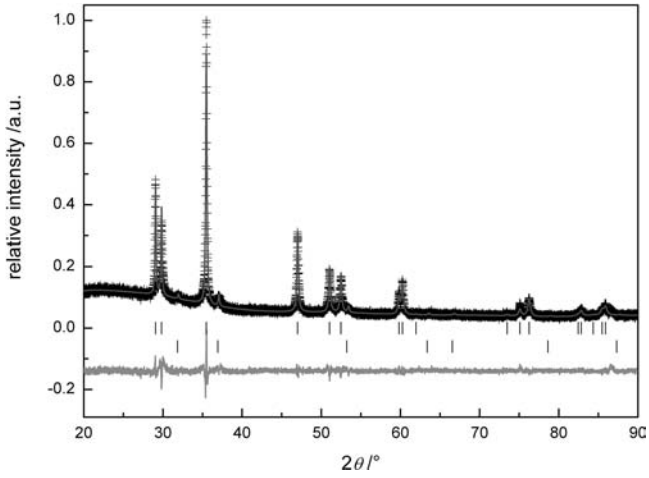

Figure 1. Observed (crosses) and calculated (gray line) powder diffraction pattern as well as difference profile of the Rietveld refinement of CaN_2; peak positions of CaN_2 (first row) and of CaO (second row; side phase) are marked by vertical lines.

Temperature-Dependent *in Situ* X-ray Diffractometry. *In situ* X-ray powder diffraction data were collected with a STOE Stadi P powder diffractometer (Mo Kα_1 radiation (0.7093 Å)) equipped with a computer controlled STOE resistance graphite furnace. Enclosed in a silica glass capillary under argon, the samples were heated from room temperature to 900 °C at a rate of 5 °C/min in steps of 25 °C. At each heating step (after holding the temperature for 1 min), a diffraction pattern was recorded with an IP-PSD in the range of $2° \leq 2\theta \leq 80°$.

Infrared Spectroscopy. Fourier transform infrared (FTIR) measurements were carried out on a Bruker IFS 66v/S spectrometer. Spectra of the samples were recorded in an evacuated cell at ambient conditions between 400 and 4000 cm^{-1} after diluting the samples in KBr pellets (2 mg sample, 300 mg KBr, pressed with 10 kN).

Calculation of the Electronic Structure. The LMTO method in its scalar relativistic version (TB-LMTO-ASA program)[41] was used to perform the calculation of the band structure, electronic density of states (DOS) and crystal orbital Hamiltonian population (COHP) of CaN_2 and SrN_2.[42] Detailed descriptions of the method are given elsewhere.[43,44] The k point set was extended to a 24 × 24 × 24 array to properly describe the metallic compounds. The basis sets consisted of Ca, 4s/{4p}/3d, Sr, 5s/{5p}/4d/{4f}, and N, 2s/2p/{3d}, where orbitals given in brackets were downfolded.[45] The electronic structure calculations converged when the change of the total energy was smaller/equal to 10^{-5} Ry. The COHP method was used for bond analysis. COHP gives the energy contributions of all electronic states for a selected bond. The values are negative for bonding and positive for antibonding interactions. With respect to the COHP diagrams, we plot −COHP(E) to obtain positive values for bonding states. The structural parameters were taken from the Rietveld refinements. The orbital character of the bands was analyzed using the so-called fat-band plots. Magnetic susceptibility measurements and electronic structure calculations for BaN_2 already revealed that the compound exhibits Pauli paramagnetism and should be metallic, despite the paramagnetic triplet state of the diazenide ion.[11] Therefore, a test spin-polarized calculation with nonzero magnetic moments artificially placed on the nitrogen atoms of CaN_2 and SrN_2 was performed and converged also back to the metallic state.

dx.doi.org/10.1021/ic2023677 | *Inorg. Chem.* 2012, 51, 2366−2373

Table 1. Synthesis Conditions and Crystallographic Data for CaN_2, SrN_2 and BaN_2

	CaN_2	SrN_2	BaN_2
synthesis conditions	12 GPa @ 800 °C	9 GPa @ 550 °C	3 GPa @ 450 °C
multianvil assembly	14/8	18/11	18/11
fw/g·mol^{-1}	68.0914	115.6334	165.3534
space group	*I*4/*mmm* (no. 139)	*I*4/*mmm* (no. 139)	*C*2/*c* (no. 15)
cell params /Å, deg	a = 3.5747(6)	a = 3.8054(2)	a = 7.1608(4)
	c = 5.9844(9)	c = 6.2961(4)	b = 4.3776(3)
			c = 7.2188(4)
			β = 104.9679 (33)
V/Å^3	76.47(3)	91.17(1)	218.61(2)
Z/cell	2	2	4
ρ_{calc}/g·cm^{-3}	2.9572(10)	4.212(1)	5.0237(5)
μ_{calc}/mm^{-1}	30.622(11)	37.068(1)	17.73(2)
d_{NN}/Å	1.202(4)	1.239(4)	1.23(2)
Data Collection			
type of diffractometer	STOE Stadi P		
geometry	Debye–Scherrer		
radiation, monochromator	Cu Kα_1 (λ = 1.54056 Å), Ge(111)	Mo Kα_1 (λ = 0.7093 Å), Ge(111)	
T/°C	25(2)		
detector	linear PSD ($\Delta 2\theta$ = 5°)		
2θ range/deg	10–90	5–90	2–80
no. of obsd reflns	17	19	690
Structure Analysis and Refinement			
meth of refinement	fundamental parameter model		
program package	TOPAS Academic		
atomic parameters	3	3	6
background function/ params	shifted Chebyshev/9	shifted Chebyshev/ 12	shifted Chebyshev/ 15
R indices	GoF(χ^2) = 1.200	GoF(χ^2) = 1.740	GoF(χ^2) = 1.495
	R_p = 0.062	R_p = 0.044	R_p = 0.037
	wR_p = 0.078	wR_p = 0.057	wR_p = 0.049

RESULTS AND DISCUSSION

Crystal Structure Elucidation of CaN_2 and SrN_2. Both alkaline earth diazenides crystallize in the same structure type, which is isotypic with the corresponding alkaline earth acetylenides ($M_{AE}C_2$), namely, in a tetragonally distorted NaCl-type. Therefore, they can be topologically derived from Sr_2N (*anti*-$CdCl_2$-type) by occupying all octahedral voids made up by the strontium ions with $[N_2]^{2-}$ units aligned along [001]. Figure 2 represents a top view of the resulting unit cell of

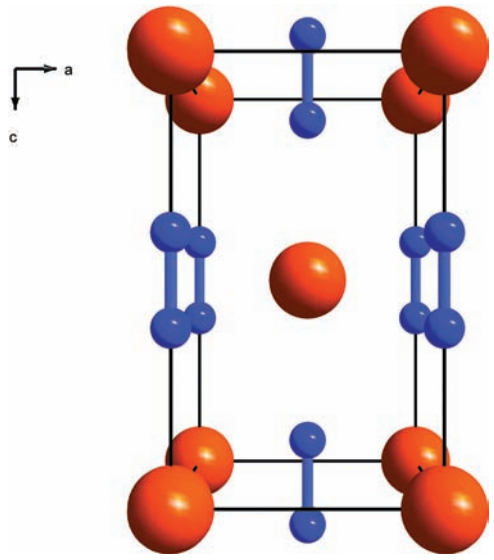

Figure 2. Top view of the unit cell of CaN_2 and SrN_2 along [010] (Ca^{2+}/Sr^{2+}, orange; nitrogen, blue).

$M_{AE}N_2$ (M_{AE} = Ca, Sr) in the (101) plane. The alkaline earth ion is coordinated "side-on" by four and "end-on" by two diazenide units (Figure 3), giving a coordination number of 8 + 2 = 10. The dinitrogen unit occupies the octahedral voids and is coordinated by six M_{AE}^{2+} ions. The occupied octahedrons are connected to each other by shared edges and faces. The experimentally found N–N bond length of SrN_2 synthesized by

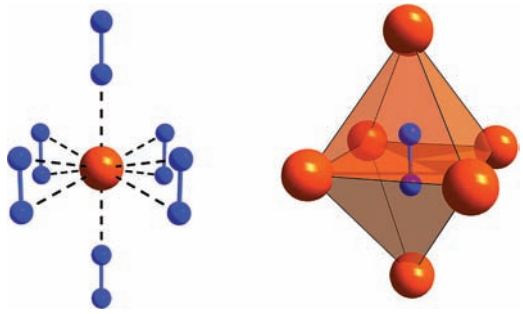

Figure 3. Coordination spheres of Sr^{2+}/Ca^{2+} on the left, and of the diazenide on the right (Ca^{2+}/Sr^{2+}, orange; nitrogen, blue).

Table 2. Refined Atomic Coordinates and Isotropic Displacement Parameters (in 0.01 Å^2) for CaN_2, SrN_2 and BaN_2

atoms	Wyckoff	x	y	z	$U_{iso}{}^a \times 100$
			CaN_2		
Ca1	2a	0	0	0	3.926(96)
N1	4e	0	0	0.3995(5)	6.15(15)
			SrN_2		
Sr1	2a	0	0	0	3.733(57)
N1	4e	0	0	0.4016(4)	2.60(13)
			BaN_2		
Ba1	4e	0	0.2006(2)	1/4	1.413(21)
N1	8f	0.3023(18)	0.1547(39)	0.0508(19)	1.99(13)

$^a U_{iso} = B_{eq}/(8\pi^2)$.

dx.doi.org/10.1021/ic2023677 | *Inorg. Chem.* 2012, 51, 2366–2373

Kniep et al. was 1.224(2) Å.[10] Here, we find a distance between the nitrogen atoms of 1.202(4) Å in CaN_2 and 1.239(4) Å in SrN_2, which is in good agreement with the former results.

As already mentioned, Wessel et al. have predicted the crystal structures of all alkaline earth diazenides theoretically.[29] For their theoretical investigation, 15 possible structural models with atomic ratio cation to anion of 1:2 were taken into account and thereby the ground-state structures predicted. The calculations confirm that the experimentally found structures for SrN_2 and BaN_2 are minimum energy structures, thus being the thermodynamically most stable structures. For CaN_2, however, the search for a plausible thermodynamic ground-state structure resulted basically in five possible structure types

Table 3. Total Energies and Molar Volumes of Predicted Ground-State Structures for CaN_2 Taken from Wessel et al.[29]

structure type	E_{total} (kJ/mol)	V (cm^3/mol)
$ZnCl_2$	−1950.0	25.04
ZrO_2	−1950.0	25.07
$PbCl_2$	−1949.8	23.54
TiO_2 (brookite)	−1949.8	23.57
CaC_2	−1949.0	23.63

(Table 3) within a tolerance of ΔE_{total} = 1 kJ/mol relative to $ZnCl_2$.

For the reported $ZnCl_2$ structure type, the authors additionally analyzed the common crystallographic details (space group, lattice parameters, atomic positions, interatomic N−N distance). In this structural model, the cations are coordinated by four dinitrogen units in an "end-on" and to another two units in a "side-on" mode which results in an effective coordination number of 4 + 4 = 8. The coordination sphere of the diazenide unit again is octahedral. The resulting N−N distance of 1.255 Å is in good agreement with the one experimentally found. Synthesized CaN_2 however, is of the $M_{AE}C_2$ structure type. Nevertheless, the calculations reveal that the $M_{AE}C_2$ structure type is close to the $ZnCl_2$ type in total energy (ΔE_{total} = 1 kJ/mol).

Crystal Structure Elucidation of BaN_2. BaN_2 shows a close structural relationship to the structure type of SrN_2 and CaN_2, although the strontium and barium compounds do not crystallize isotypically. In BaN_2, the metal ions also form a closed packing, in which the $[N_2]^{2-}$ ions occupy all octahedral voids (Figure 4, left). Again, edge and face sharing of octahedra results. However, due to the lower symmetry of BaN_2 compared to CaN_2 and SrN_2, the octahedral voids are occupied with nitrogen dimers aligned horizontally along the diagonals of the Ba^{2+} octahedra with alternating orientation within each layer. Only along [100], the same orientation of dinitrogen units is found. Therefore, the coordination sphere of Ba^{2+} is quite similar but slightly more distorted (Figure 4, right). Two diazenide units coordinate in an "end-on" and four $[N_2]^{2-}$ ions in a "side-on" fashion (with two different sets of distances to Ba^{2+}), thus resulting in a coordination number of 2 + 4 + 4 = 10. As expected, the experimentally found N−N bond distance of the diazenide ion 1.204(3) Å is intermediate between those of a N−N single-bond and triple-bond.

Vibrational Spectroscopy. For SrN_2 and SrN (=$(Sr^{2+})_4(N^{3-})_2([N_2]^{2-})$, a nitride-diazenide) inelastic neutron scattering (INS) spectroscopy already revealed that an observed feature at 1380 cm^{-1} (SrN) and 1307 cm^{-1} (SrN_2) can be assigned to the N−N stretching vibration of the diazenide ion.[46] Remaining features at considerably lower wavenumbers (<350 cm^{-1}) were assigned to acoustic, optic translational and librational modes of the $[N_2]^{2-}$ ion.

Concerning a free nitrogen molecule (point symmetry $D_{\infty h}$), the only fundamental vibration (Σ_g) is Raman-active and IR-inactive due to the rule of mutual exclusion.[47] However, the infrared spectra of $M_{AE}N_2$ (M_{AE} = Ca, Sr, Ba), which are shown in Figure 5, exhibit clear features at 1376.9 (CaN_2), 1378.9 (SrN_2) and 1375.9 cm^{-1} (BaN_2), which are assigned to the N−N stretching vibration of the $[N_2]^{2-}$ ion. Therefore, in comparison to the free dinitrogen molecule with only one Raman-active mode, the corresponding site symmetry of the diazenide ion in the solid has to be reduced to observe IR-active modes. This condition can be verified using the correlation method.[47] The reduced site symmetry for the dinitrogen unit in CaN_2 and SrN_2 is C_{4v}, resulting in two possible IR-active modes (A_1, E). In BaN_2, there is a $D_{\infty h} \rightarrow C_1$ reduction in symmetry with one IR- and Raman-active vibration (A). Applying the correlation method,[47] the only IR-active modes for CaN_2 and SrN_2 (factor symmetry D_{4h}) are A_{2u} and E_u, and for BaN_2 (C_{2h}) A_u and B_u. Therefore, in the corresponding crystal, the solely Raman-active mode in the free dinitrogen molecule is split into either one of those IR-active modes for the dinitrogen units, which is clearly observed in the FTIR spectra.

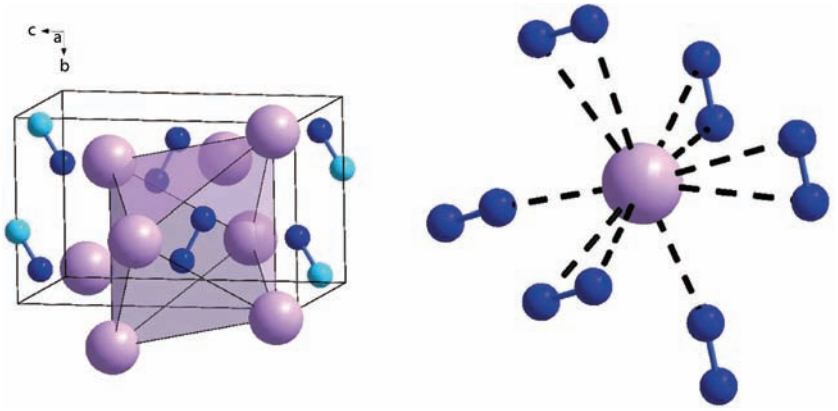

Figure 4. Unit cell of BaN_2 with coordination of the diazenide unit on the left; Ba^{2+} coordination sphere on the right (Ba^{2+}, light purple; nitrogen, blue; nitrogen not in unit cell, turquoise).

dx.doi.org/10.1021/ic2023677 | Inorg. Chem. 2012, 51, 2366−2373

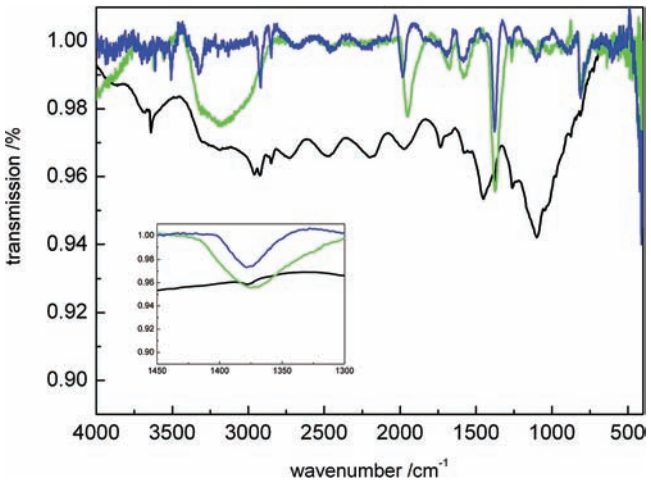

Figure 5. FTIR spectra of CaN_2 (black), SrN_2 (blue) and BaN_2 (green). The region of the $[N_2]^{2-}$ feature is enlarged (bottom left).

However, there are still a number of unidentified features, which might be caused by additional (translational, acoustic, librational) modes of the diazenide unit due to lattice distortions. On the other hand, due to the extremely high sensitivity to moisture, these compounds tend to hydrolyze very easily. As the KBr-sample pellet is exposed to normal atmosphere upon transfer from the glovebox to the sample chamber of the spectrometer, diverse intermediates could be formed resulting in a variety of possible IR vibrations due to diverse functional groups.

Our attempts to record Raman spectra failed. This may be caused by reflection or absorption of the laser by the intensely black alkaline earth diazenides.

Temperature-Dependent *in situ* X-ray Diffractometry. The temperature-dependent *in situ* X-ray diffraction patterns for CaN_2 and BaN_2 are depicted in Figure 6. The temperature-dependent *in situ* powder X-ray diffraction patterns of SrN_2 are given in Figure S1 in the Supporting Information. It is clearly seen that each alkaline earth diazenide transforms into the subnitride $M_{AE_2}N$ upon heating. For CaN_2, the temperature of transformation is about 100 °C lower (at approximately 230 °C) than for SrN_2 and BaN_2 (both at approximately 325 °C). These measurements are in good agreement with the reported value for SrN_2 of 320 °C upon heating SrN_2 in vacuum.[10,14]

It is noteworthy that all three alkaline earth diazenides react analogously forming the respective subnitrides $M_{AE_2}N$ upon heating. In the case of strontium and barium diazenide this behavior seems reasonable as the stoichiometric nitrides $M_{AE_3}N_2$ do not seem to exist.[48] In contrast, Ca_3N_2 is a stable phase. However it is not formed during thermal decomposition of CaN_2.

Electronic Structure. To better understand the electronic structure of the alkaline earth diazenides and their bonding situation, first principles calculations on the electronic structure were performed. As the band structure, density of states (DOS) and crystal orbital Hamiltonian population (COHP) of BaN_2 have already been calculated,[11,24] we here report on the electronic structure of CaN_2 and SrN_2. In Figure 7 the band structures of both diazenides are depicted. As expected, the electronic structure calculations suggest that the compound should be metallic, which is in good agreement with the observed black metallic color of the samples. In both cases, the main contributions of bands at the Fermi level comes from the M_{AE}-d (Ca, 3d; Sr, 4d) and the N-p (2p) states. The contribution of the M_{AE}-p states (Ca, 4p; Sr, 5p) is negligible.

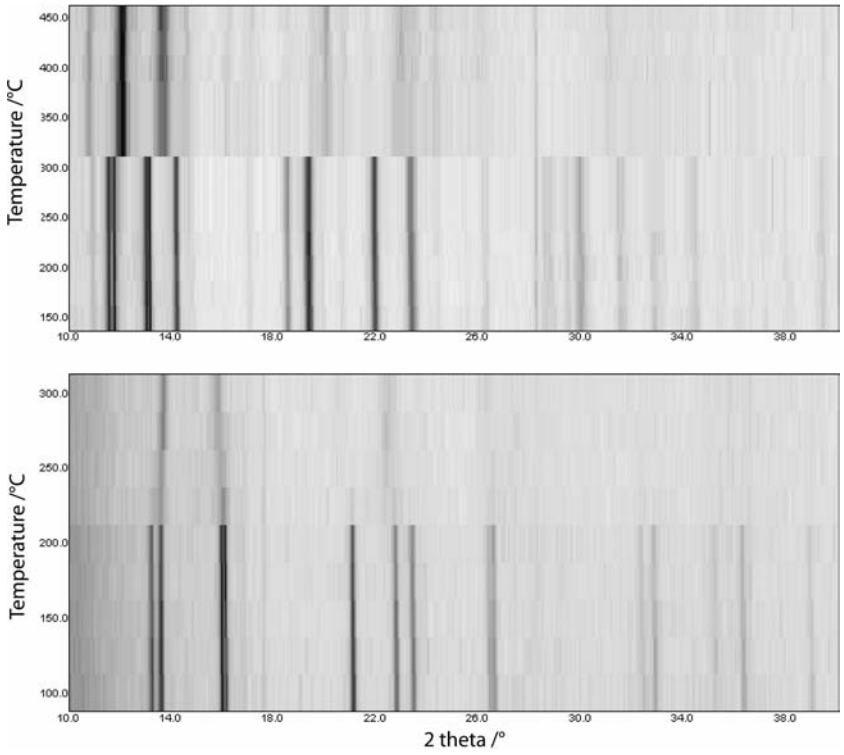

Figure 6. Temperature-dependent *in situ* X-ray powder diffraction patterns of CaN_2 (bottom) and BaN_2 (top).

dx.doi.org/10.1021/ic2023677 | *Inorg. Chem.* 2012, 51, 2366–2373

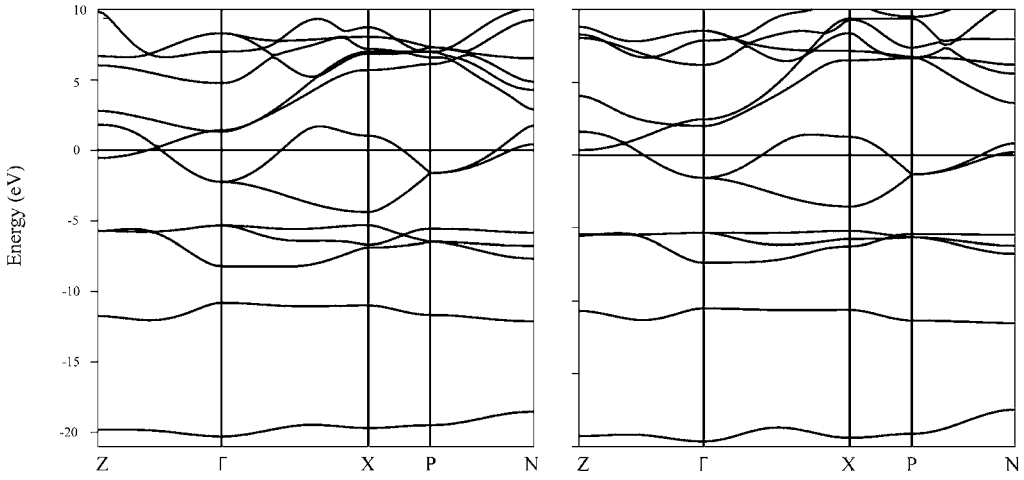

Figure 7. TB-LMTO band structures for CaN_2 (left) and SrN_2 (right).

To illustrate the bonding situation, Figure 8 displays a scheme of the molecular-orbital diagram of N_2 and $[N_2]^{2-}$.

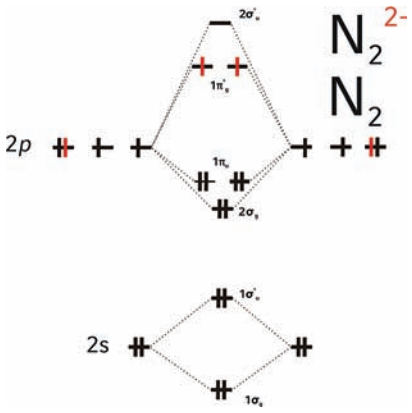

Figure 8. Molecular-orbital scheme of the dinitrogen molecule illustrating the electron filling for N_2 and $[N_2]^{2-}$.

Upon forming N_2 by linear combination of the atomic orbitals of elemental nitrogen, the molecular orbitals $1\sigma_g$, $1\sigma_u^*$, $2\sigma_g$, $1\pi_u$, $1\pi_g^*$ and $2\sigma_u^*$ are formed. The bonding orbitals $2\sigma_g$ and $1\pi_u$ are filled up with six electrons resulting in a maximum of bonding multiplicity of three (triple bond). Adding further two electrons into the $1\pi_g^*$ molecular orbital (red vertical lines in Figure 8) results on the one hand in $[N_2]^{2-}$ and on the other hand in a reduced bonding multiplicity of 2 which corresponds to the double-bonded nitrogen dimer. Notice that only 50% of the antibonding molecular orbital $1\pi_g^*$ is occupied. The $[N_2]^{2-}$ ion is isosteric to molecular oxygen and $[C_2]^{4-}$ and therefore should exhibit paramagnetic behavior. However, magnetic susceptibility measurements and electronic structure calculations for BaN_2 revealed that the compound exhibits Pauli paramagnetism and should be metallic, despite the paramagnetic triplet state of the isolated diazenide ion.[11] Thus, a test spin-polarized calculation with nonzero magnetic moments artificially placed on the nitrogen atoms was conducted for CaN_2 and SrN_2 and converged back to the metallic state. This implies that CaN_2 and SrN_2 should be metallic as well. Further addition of two electrons into the molecular-orbital scheme

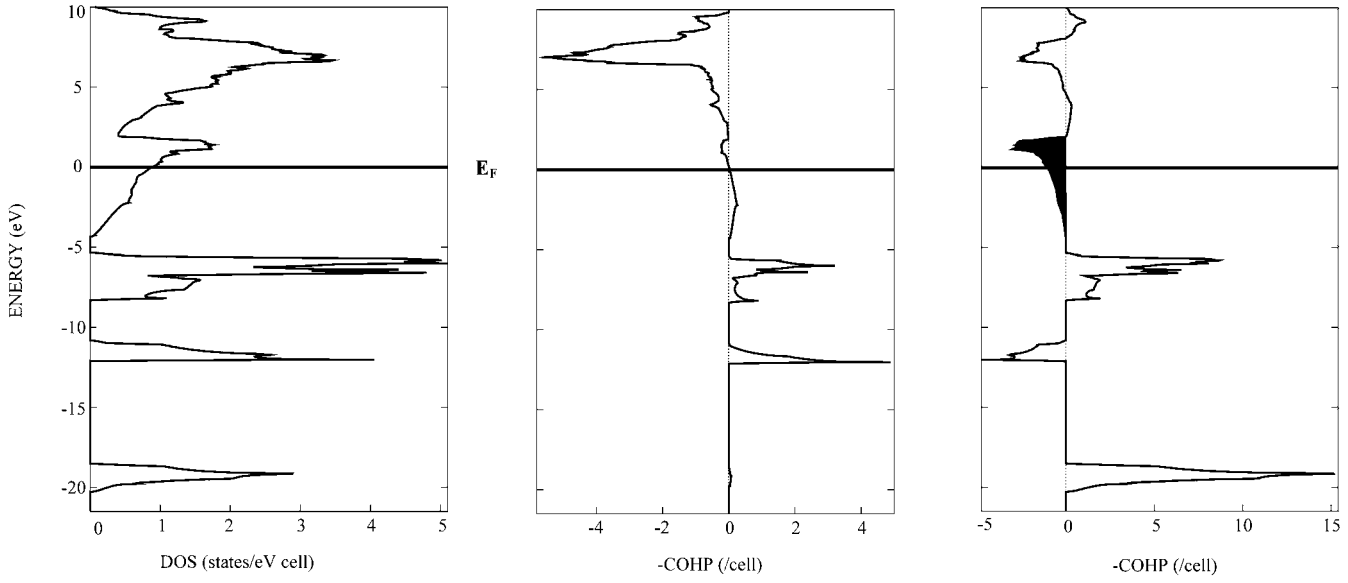

Figure 9. Total DOS (left), COHP analysis of Ca−N (middle) and N−N (right) for CaN_2.

dx.doi.org/10.1021/ic2023677 | Inorg. Chem. 2012, 51, 2366−2373

then results in $[N_2]^{4-}$ and another reduction in bonding multiplicity by 1 (single bond).

To elucidate the bonding situation in CaN_2 and SrN_2, the DOS and COHP (M_{AE}–N and N–N) were calculated and are depicted in Figure 9 (CaN_2) and Figure S2 in the Supporting Information (SrN_2). In the COHP plots, the bonding states are given as features to the right, whereas antibonding states show up as features to the left. Since they share the same space groups and crystal structures, the situation for both alkaline earth diazenides is basically the same. The bonding states at about −20 eV are mainly based on the $1\sigma_s$ orbitals of the dumbbell. At about −12 eV the dinitrogen $1\sigma_u$* states can be found mixing with M_{AE}-s, -p and -d states (Ca, 4s, 4p, 3d; Sr, 5s, 5p, 4d). Above that, around −8 to −5 eV the $2\sigma_g$ and the $1\pi_u$ states of the dinitrogen unit show up as bonding states together with an increased contribution of the M_{AE}-d states and a decreased one of the M_{AE}-p and -s states. The antibonding bands in the proximity of the Fermi level ranging from −4 to 2 eV are found to be basically built up by the $1\pi_g$* states of the dinitrogen unit, which are slightly mixed with the M_{AE}-s and -d states. These metal–nitrogen interactions are found to be responsible for the significant widths of the corresponding bands in the band structure, and thus probably are also responsible for the metallic character of these compounds. The bands above 2 eV are predominantly formed by M_{AE}-d states. For the M_{AE}–N combination (Figure 9, middle; Figure S2 in the Supporting Information, middle), there are basically only bonding states up to E_F. Above the Fermi level (in the region of the unoccupied states), the antibonding M_{AE}–N interactions are observed. The COHP plots of the N–N combination (Figure 9, right; Figure S2 in the Supporting Information, right) in the range of −4 to 2 eV are clearly dominated by antibonding states where the Fermi level crosses these states at about half of their antibonding character. This perfectly matches with the expected 50% occupation of the antibonding π-states of the diazenide ion $[N_2]^{2-}$.

CONCLUSIONS

By controlled decomposition of the alkaline earth azides of calcium, strontium and barium, the corresponding diazenides $M_{AE}N_2$ (M_{AE} = Ca, Sr, Ba) were synthesized in accord with the pressure-homologue rule (isotypic structures with the heavier homologues can be synthesized by lower pressure; lighter homologues: higher pressure). FTIR spectroscopy of these diazenides resulted in a band at about 1380 cm^{-1} assigned to the N–N strechting vibration of the diazenide ion. Temperature-dependent *in situ* powder X-ray diffraction revealed that CaN_2, SrN_2 and BaN_2 transformed into the corresponding subnitrides $M_{AE_2}N$ at higher temperatures. To better understand the bonding situation in the diazenides, electronic structure calculations were performed for CaN_2 and SrN_2. As expected, the diazenides show metallic behavior (DOS). In addition, COHP calculations revealed a 50% occupation of the antibonding π-states of the diazenide ion and therefore support the formulation of a double-bonded, 2-fold negatively charged $[N_2]^{2-}$ ion.

ASSOCIATED CONTENT

Supporting Information

Temperature-dependent *in situ* X-ray powder diffraction patterns, DOS and COHP (Sr–N, N–N) of SrN_2. This material is available free of charge via the Internet at http://pubs.acs.org.

AUTHOR INFORMATION

Corresponding Author

*E-mail: wolfgang.schnick@uni-muenchen.de. Phone: (+49) 89-2180-77436. Fax: (+49)89-2180-77440.

ACKNOWLEDGMENTS

We gratefully acknowledge financial support by the Fonds der Chemischen Industrie FCI and the Deutsche Forschungsgemeinschaft DFG (Project SCHN377/13-2). The authors thank Prof. Dirk Johrendt for valuable discussion.

REFERENCES

(1) Matoba, G. Patent JP-B 50010804, 1975. Matoba, G. Patent JP-B 50010803, 1975. Kobayashi, H. Patent JP-A 03006314, 1991. Chokei, T. Patent JP 55094432, 1980. Willners, H. Patent SE 115621, 1946.
(2) Jhi, S. H.; Ihm, J.; Louie, S. G.; Cohen, M. L. *Nature* **1999**, *399*, 132–134.
(3) McMillan, P. F. *Nat. Mater.* **2002**, *1*, 19–25.
(4) Maruyama, T.; Morishita, T. *Appl. Phys. Lett.* **1996**, *69*, 890–891.
(5) Yamanaka, S.; Hotehama, K.; Kawaji, H. *Nature* **1998**, *392*, 580–582.
(6) Zerr, A.; Miehe, G.; Boehler, R. *Nat. Mater.* **2003**, *2*, 185–189.
(7) Chhowalla, M.; Unalan, H. E. *Nat. Mater.* **2005**, *4*, 317–322.
(8) Leineweber, A.; Jacobs, H.; Hull, S. *Inorg. Chem.* **2001**, *40*, 5818–5822.
(9) Wu, Z. G.; Chen, X. J.; Struzhkin, V. V.; Cohen, R. E. *Phys. Rev. B* **2005**, *71*, 214103.
(10) Auffermann, G.; Prots, Y.; Kniep, R. *Angew. Chem.* **2001**, *113*, 565–567; *Angew. Chem., Int. Ed.* **2001**, *40*, 547–549.
(11) Vajenine, G. V.; Auffermann, G.; Prots, Y.; Schelle, W.; Kremer, R. K.; Simon, A.; Kniep, R. *Inorg. Chem.* **2001**, *40*, 4866–4870.
(12) Auffermann, G.; Schmidt, U.; Bayer, B.; Prots, Y.; Kniep, R. *Anal. Bioanal. Chem.* **2002**, *373*, 880–882.
(13) Auffermann, G.; Kniep, R.; Bronger, W. *Z. Anorg. Allg. Chem.* **2006**, *632*, 565–571.
(14) Prots, Y.; Auffermann, G.; Tovar, M.; Kniep, R. *Angew. Chem.* **2002**, *114*, 2392–2394; *Angew. Chem., Int. Ed.* **2002**, *41*, 2288–2290.
(15) Gregoryanz, E.; Sanloup, C.; Somayazulu, M.; Badro, J.; Fiquet, G.; Mao, H.-K.; Hemely, R. J. *Nat. Mater.* **2004**, *3*, 294–297.
(16) von Appen, J.; Lumey, M.-W.; Dronskowski, R. *Angew. Chem.* **2006**, *118*, 4472–4476; *Angew. Chem., Int. Ed.* **2006**, *45*, 4365–4368.
(17) Crowhurst, J. C.; Goncharov, A. F.; Sadigh, B.; Evans, C. L.; Morrall, P. G.; Ferreira, J. L.; Nelson, A. J. *Science* **2006**, *311*, 1275–1278.
(18) Young, A. F.; Montoya, J. A.; Sanloup, C.; Lazzeri, M.; Gregoryanz, E.; Scandolo, S. *Phys. Rev. B* **2006**, *73*, 153102.
(19) Montoya, J. A.; Hernandez, A. D.; Sanloup, C.; Gregoryanz, E.; Scandolo, S. *Appl. Phys. Lett.* **2007**, *90*, 011909.
(20) Crowhurst, J. C.; Goncharov, A. F.; Sadigh, B.; Zaug, J. M.; Aberg, D.; Meng, Y.; Prakapenka, V. B. *J. Mater. Res.* **2008**, *23*, 1–5.
(21) Chen, Z. W.; Guo, X. J.; Liu, Z. Y.; Ma, M. Z.; Jing, Q.; Li, G.; Zhang, X. Y.; Li, L. X.; Wang, Q.; Tian, Y. J.; Liu, R. P. *Phys. Rev. B* **2007**, *75*, 054103.
(22) Yu, R.; Zhan, Q.; De Jonghe, L. C. *Angew. Chem.* **2007**, *119*, 1154–1158; *Angew. Chem., Int. Ed.* **2007**, *46*, 1136–1140.
(23) Chen, W.; Tse, J. S.; Jiang, J. Z. *J. Phys.: Condens. Matter* **2010**, *22*, 015404.
(24) Wessel, M.; Dronskowski, R. *J. Am. Chem. Soc.* **2010**, *132*, 2421–2429.
(25) Wessel, M.; Dronskowski, R. *Chem.—Eur. J.* **2011**, *17*, 2598–2603.
(26) Wessel, M. PhD thesis, RWTH Aachen University, Aachen, 2010.

(27) Du, X. P.; Wang, Y. X.; Lo, V. C. *Phys. Lett. A* **2010**, *374*, 2569−2574.
(28) Wang, H.; Li, Q.; Li, Y.; Xu, Y.; Cui, T.; Oganov, A. R.; Mal, Y. *Phys. Rev. B* **2009**, *79*, 132109.
(29) Wessel, M.; Dronskowski, R. *J. Comput. Chem.* **2010**, *31*, 1613−1617.
(30) Frierson, W. J. *Inorg. Synth.* **1946**, *8*, 136−138.
(31) Fair, H. D.; Walker, R. F. *Energetic Materials Vol. 1: Physics and Chemistry of the Inorganic Azides*; Plenum Press: New York, 1977.
(32) Ehrlich, P.; Seifert, H. J; Brauer, G. *Handbuch der Präparativen Anorganischen Chemie Vol. 2*; Ferdinand Enke Verlag: Stuttgart, 1978.
(33) Remy-Gennete, P. *Ann. Chim.* **1933**, *19*, 289−291.
(34) Walker, D.; Carpenter, M. A.; Hitch, C. M. *Am. Mineral.* **1990**, *75*, 1020−1028.
(35) Walker, D. *Am. Mineral.* **1991**, *76*, 1092−1100.
(36) Huppertz, H. *Z. Kristallogr.* **2004**, *219*, 330−338.
(37) Rubie, D. C. *Phase Transitions* **1999**, *68*, 431−451.
(38) Kawai, N.; Endo, S. *Rev. Sci. Instrum.* **1970**, *8*, 1178−1181.
(39) Coelho, A. A. *TOPAS-Academic*, Version 4.1; Coelho Software: Brisbane, 2007.
(40) Bergmann, J.; Kleeberg, R.; Haase, A.; Breidenstein, B. *Mater. Sci. Forum* **2000**, *303*, 347−349.
(41) Andersen, O. K.; Jepsen, O. *Tight-Binding LMTO Vers. 4.7*; Max-Planck-Institut für Festkörperforschung: Stuttgart, 1994.
(42) Dronskowski, R.; Blöchl, P. *J. Phys. Chem.* **1993**, *97*, 8617−8624.
(43) Jepsen, O.; Snob, M.; Andersen, O. K. *Linearized Band Structure Methods and its Applications*; Springer Lecture Notes; Springer-Verlag: Berlin, 1987.
(44) Skriver, H. L. *The LMTO Method*; Springer-Verlag: Berlin, 1984.
(45) Lambrecht, W. R. L.; Andersen, O. K. *Phys. Rev. B* **1986**, *34*, 2439−2449.
(46) Auffermann, G.; Prots, Y.; Kniep, R.; Parker, S. F.; Bennington, S. M. *Chem. Phys. Chem.* **2002**, *9*, 815−817.
(47) Weidlein, J.; Müller, U.; Dehnicke, K. *Schwingungsspektroskopie − Eine Einführung*; Georg Thieme Verlag: Stuttgart, New York, 1982.
(48) Römer, S. R.; Dörfler, T.; Kroll, P.; Schnick, W. *Phys. Status Solidi B* **2009**, *246*, 1604−1613.